High Dynamic Digital Control for a Hydraulic Cylinder Drive*

Helmut Kogler

Linz Center of Mechatronics.

Altenberger Strasse 69
4040 Linz, Austria.
helmut.kogler@lcm.at

Abstract

The control of hydraulic cylinders with digital hydraulic valves is often based on modulation principles like pulse-width-modulation, pulse-code-modulation or pulse-frequency-control. In many cases the dynamic drive performance using such control strategies is far below the natural dynamics of the system, since closed loop controllers demand a certain phase margin for stability. However, some drive applications require a high dynamic response, which cannot be realized with common closed loop concepts. In this paper the design of a bang-bang feedforward control with regard to the dynamics of a hydraulic cylinder drive in accordance with the theory of optimal control is presented. The control achieves the maximum physical dynamic response and no remaining oscillations after the movement, which forms the basis of a high dynamic three-level position control for hydraulic drives. Furthermore, the influence of valve dynamics and pipe line dynamics with regard to the design of the digital valve control are considered by simulations.

Keywords: digital, hydraulics, high dynamic, switching control

1 Introduction

In digital hydraulic drives simple on/off valves are used for the control of the actuator. Due to their simple design, digital valves are far less expensive than proportional valves, or even servo valves. Furthermore, since digital valves have only two switching states, either open or closed, such valves are also more robust against oil contamination compared to for instance servo valves. However, in many cases unwanted vibrations are caused by the switching of the valves, since inertial loads in combination with the compressibility of the fluid result in weakly damped oscillatory systems. Therefore, certain switching strategies must be applied in order to achieve the desired motion and, in turn, to avoid the excitation of unwanted resonances. So far, in hydraulics the following different methods in digital valve control have been established:

In Pulse-Code-Modulation (PCM) the flow rate for the intended motion of the drive is controlled by different digital valves arranged in parallel and often of different sizes. Thus, the flow through the valve is coded by certain combinations of the different valves (see, for instance, [1, 2, 3]). The requirements on the switching times of the valves do not play a significant role unless two or more valves are intended to be switched at the same time. In such a case a perfect synchronous switching of the valves is necessary in order to avoid pressure fluctuations due to an undesirable effective valve opening. A main advantage of this concept is the reliability due to the parallel arrangement of several valves, i.e. in case of one faulty valve the drive is still able to operate at reduced performance. Drawbacks of this method are the high number of valves and the complicated programming of the control unit, especially when fault detection is implemented.

The concept of Pulse-Width-Modulation (PWM) uses a constant frequency for the switching of the digital valves. The mean flow rate through a valve is controlled by the duty ratio between the on- and offtime of the valve within the switching period, see for instance [4, 5, 6, 7, 8]. Furthermore, this method is often used in energetically efficient

*Proceedings of the IMechE, Part I: Journal of Systems and Control Engineering, Accepted Version, July, 2021. DOI: 10.1177/09596518211028089

hydraulic step-down switching converters as presented in [9, 10, 11, 12]. Moreover, in [13] the PWM switching strategy is used in a hydraulic step-up converter in order to boost the load pressure. However, in order to achieve a smooth movement of the drive, the switching frequency is required to be much higher than the natural frequency of the drive. Due to the limited switching frequencies in hydraulics (see e.g. [14]) in some cases the drive dynamics must be even slowed down by gas-loaded attenuation devices, which in turn results often in an unwanted soft hydraulic drive system.

Another method in digital hydraulic valve control is the so called Pulse-Frequency-Control (PFC). The velocity of the drive is controlled by the frequency of a well defined single flow pulse. Such a pulse does not need to be produced by a digital valve rather, for instance, by a magnetically actuated piston pump. A basic study of this concept for hydraulic systems can be found, for instance, in [15]. The PFC is designed to the dynamics of the drive in order to keep the unwanted oscillations low. Therefore, the pulses must be produced in a certain phase relation with regard to the natural frequency of the drive.

In [16, 17] strategies for an optimal feedforward control of digital hydraulic drives are presented. The considerations were based on optimal control theory, however, they were focused on numerical investigations. Furthermore, due to the structure of the models the resulting calculation effort for the numeric analysis was quite high. Moreover, in many cases the presented numeric control is not realized by a strict digital valve opening, but by a sort of proportional valve openings.

In this paper a simple analytical bang-bang control strategy named High Dynamic Digital Control (HDDC) for a hydraulic cylinder with a dead load is presented, which results in the maximum dynamic response and, moreover, minimizes remaining oscillations excited by the digital switching process. The control is designed with regard to the natural frequency of the hydraulic drive in order to achieve maximum acceleration and deceleration of the load. For this purpose the valves are actuated in the correct phase angle of the relevant natural frequency of the system, which results in the mentioned high dynamic response at minimized remaining oscillations at the end of the trajectory. In case of only one natural frequency no resonances will remain after the intended movement. Like in other mentioned literature, the design of the HDDC is based on optimal control theory, in particular, on Pontryagin's Maximum Principle according to, e.g. [18]. In fact, the feedforward control derived in this paper leads to similar results as from input-shaping techniques like, for instance [19, 20], however, in contrast to the lastly mentioned literature the considerations in this paper give deep insight into the physics of digitally actuated drives.

The paper is organized as follows: In Section 2 the modeling and the mathematical design of the HDDC are considered. In Section 3 a number of simulation results with regard to the basic operating principle of the HDDC are presented. Furthermore, advanced simulations regarding nonideal effects like valve switching times, pipe line dynamics and friction are illustrated in the same section. A comprehensive discussion is given in Section 4 and finally an outlook to future work is provided in Section 5.

2 High Dynamic Digital Control

The digital valve control presented in the following is a model based control, which needs knowledge of the system dynamics. For this purpose a mathematical model is necessary, which is presented in the following subsection. The concept of the HDDC is a bang-bang control strategy based on Pontryagin's Minimum (Maximum) principle according to optimal control theory.

2.1 Modelling

In this paper the design of the HDDC is focused on a linear hydraulic drive according to Fig. 1. In order to keep the calculations simple no pipe line between the cylinder and the valves is considered and, furthermore, the cylinder is operated in plunger mode, which means that the annulus chamber is connected to supply pressure, permanently. The resulting nonlinear differential equa-

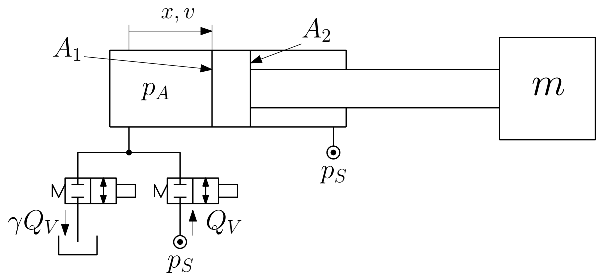

Fig. 1: Differential cylinder in plunger mode

tions read

$$\begin{aligned} \dot{x} &= v \\ \dot{v} &= \frac{1}{m}\left(p_A A_1 - p_S A_2 - d_v v\right) \\ \dot{p}_A &= \frac{E}{V_0 + A_1 x}\left(-A_1 v + Q_V u\right) \end{aligned} \quad (1)$$

with the states x and v for the piston's position and velocity and p_A the pressure in the cylinder chamber. The parameters are the dead load m, the cross-section areas of the piston A_1 and A_2, the fluid volume in the cylinder chamber V_0 and the modulus of compressibility of the fluid E. For simplicity no additional load force and, furthermore, zero-gravity are considered, which results in an equilibrium pressure $\overline{p_A} = \frac{A_2}{A_1} p_S$. Moreover, the pressure fluctuations due to a rapid movement of the dead load are assumed to be small, which means that the ratio between the cross-section area A_1 and the dead load m is correspondingly large. The input of the system is a digital flow rate with $Q_V = Q_N \sqrt{\frac{\Delta p}{p_N}} \approx$ const., and $u \in [-\gamma, 0, 1]$. The input $u = 1$ means that a supply sided digital valve is switched on. The parameter $\gamma \geq 0$ represents an additional degree of freedom with the meaning of a tank sided valve with a scaled flow of γ with respect to the flow through the supply sided valve. Moreover, with the parameterization γ different valve sizes and, moreover, different pressure drops Δp can be considered. From the starting point of view the assumption of a constant Q_V is justified, since a digital valve gains a constant flow rate as far as the pressure drop and, thus, the pressure in the cylinder is nearly constant. On the one hand, this is fulfilled by the assumptions of a large pressure drop at the valve and, furthermore, of small pressure fluctuations of p_A due to the switching. On the other hand, a constant supply pressure is required, which cannot be assumed in general at fast valve switching processes, since limited dynamics of the pressure supply system must be expected. However, with decoupling accumulators, which are installed close to the supply sided ports of the switching valves, unwanted fluctuations of the supply pressure can be prevented.

The system (1) is nonlinear, which hinders a simple design of the HDDC. A numerical analysis is not intended in the considerations because then the insight to the dynamic behaviour of the systems is not clear. Thus, the nonlinear system is linearized along a rest position. Furthermore, the viscous damping coefficient d_v is usually not known for real drive systems. However, it is assumed that in most cases the friction in the system does not significantly influence the natural frequency of the drive system. Thus, for simplicity the friction is neglected in the design process. In this case the control is designed to a completely undamped system and in reality the actual friction maintains a reduction of unwanted oscillations. Furthermore, it is assumed that during acceleration and deceleration the displacement volume due to the piston movement is small, which leads to $V_C = V_0 + A_1 x \approx$ const. With these assumptions the system (1) can be linearized to

$$\dot{\mathbf{x}} = \underbrace{\begin{bmatrix} 0 & 1 & 0 \\ 0 & 0 & \frac{1}{\alpha} \\ 0 & -\beta & 0 \end{bmatrix}}_{\mathbf{A}} \mathbf{x} + \underbrace{\begin{bmatrix} 0 \\ 0 \\ \delta \end{bmatrix}}_{\mathbf{b}} u \quad (2)$$

with $\alpha = \frac{m}{A_1}$, $\beta = \frac{EA_1}{V_C}$ and $\delta = \frac{EQ_V}{V_C}$ and the state vector $\mathbf{x} = \begin{bmatrix} \Delta x & \Delta v & \Delta p_A \end{bmatrix}^\intercal = \begin{bmatrix} x_1 & x_2 & x_3 \end{bmatrix}^\intercal$. The linearized system (2) is controllable due to

$$\begin{aligned} &\operatorname{rank}\left([\mathbf{b}, \mathbf{A}.\mathbf{b}, \mathbf{A}.\mathbf{A}.\mathbf{b}]\right) = \\ &\operatorname{rank}\left(\begin{bmatrix} 0 & 0 & \frac{\delta}{\alpha} \\ 0 & \frac{\delta}{\alpha} & 0 \\ \delta & 0 & -\frac{\beta\delta}{\alpha} \end{bmatrix}\right) = 3, \end{aligned} \quad (3)$$

has the eigenvalues $\omega_{1,2,3} = \left[0, \pm\sqrt{-\frac{\beta}{\alpha}}\right]$ and will be used for the design of the HDDC as shown in the following.

2.2 Optimal Control

The intention is to design a bang-bang control in order to accelerate the drive according Fig. 1

within the shortest time $T^\star$ from an equilibrium point to maximum velocity, thus

$$\mathbf{x}_0 = \begin{bmatrix} 0 & 0 & 0 \end{bmatrix}^\mathsf{T} \text{ and} \quad (4)$$

$$\mathbf{x}(T^\star) = \begin{bmatrix} x_1 & \frac{\delta}{\beta} & 0 \end{bmatrix}^\mathsf{T} \quad (5)$$

with δ/β as the quotient of the input flow coefficient and the cross-section area of the piston, i.e. the steady state velocity. Since the system (2) is linear, it is clear that an exchange of initial and end conditions leads to a control, which decelerates the drive from steady state velocity to equilibrium. This is also valid for the opposite moving direction.

The analytic solution of the differential equation (2) reads

$$\begin{aligned} x_1 &= \sqrt{\frac{\alpha}{\beta}}\left(\frac{\sin\left(\sqrt{\frac{\beta}{\alpha}}t\right)(\beta x_{20}-\delta u_0)}{\beta} - \frac{\cos\left(\sqrt{\frac{\beta}{\alpha}}t\right)x_{30}}{\sqrt{\alpha\beta}}\right) + \frac{x_{30}+\delta u_0}{\beta} + x_{10} \\ x_2 &= \frac{\sin\left(\sqrt{\frac{\beta}{\alpha}}t\right)x_{30}}{\sqrt{\alpha\beta}} + \frac{\cos\left(\sqrt{\frac{\beta}{\alpha}}t\right)(\beta x_{20}-\delta u_0)}{\beta} + \frac{\delta}{\beta}u_0 \quad (6) \\ x_3 &= \sqrt{\alpha\beta}\left(\frac{\cos\left(\sqrt{\frac{\beta}{\alpha}}t\right)x_{30}}{\sqrt{\alpha\beta}} - \frac{\sin\left(\sqrt{\frac{\beta}{\alpha}}t\right)(\beta x_{20}-\delta u_0)}{\beta}\right) \end{aligned}$$

with the initial conditions x_{10}, x_{20}, x_{30} and the input u_0. According to the theory of optimal control (see, for instance, [18]) the Hamiltonian follows to

$$\begin{aligned} H &= 1 + \lambda^\mathsf{T}(\mathbf{A}\mathbf{x} + \mathbf{b}u) \\ &= 1 + \lambda_1 x_2 + \frac{\lambda_2 x_3}{\alpha} + \lambda_3(-\beta x_2 + \delta u) \quad (7) \end{aligned}$$

with the adjoint differential equations ($\dot{\boldsymbol{\lambda}}^\mathsf{T} = -\frac{\partial H}{\partial \mathbf{x}}$)

$$\begin{bmatrix} \dot\lambda_1 \\ \dot\lambda_2 \\ \dot\lambda_3 \end{bmatrix} = \begin{bmatrix} 0 & 0 & 0 \\ -1 & 0 & \beta \\ 0 & -\frac{1}{\alpha} & 0 \end{bmatrix} \begin{bmatrix} \lambda_1 \\ \lambda_2 \\ \lambda_3 \end{bmatrix}. \quad (8)$$

The general solution of Eq. (8) calculates to

$$\begin{aligned} \lambda_1 &= C_1 \\ \lambda_2 &= \sqrt{\alpha\beta}\left(\sin\left(\sqrt{\frac{\beta}{\alpha}}t\right)C_2 - \cos\left(\sqrt{\frac{\beta}{\alpha}}t\right)C_3\right) \\ \lambda_3 &= \sin\left(\sqrt{\frac{\beta}{\alpha}}t\right)C_3 + \cos\left(\sqrt{\frac{\beta}{\alpha}}t\right)C_2 + \frac{C_1}{\beta}. \end{aligned}$$

With regard to theory the roots of the expression

$$\begin{aligned} \sigma &= \boldsymbol{\lambda}^\mathsf{T}\mathbf{b} = \begin{bmatrix} \lambda_1 & \lambda_2 & \lambda_3 \end{bmatrix} \cdot \begin{bmatrix} 0 \\ 0 \\ \delta \end{bmatrix} \\ &= \left(\sin\left(\sqrt{\frac{\beta}{\alpha}}t\right)C_3 + \cos\left(\sqrt{\frac{\beta}{\alpha}}t\right)C_2 + \frac{C_1}{\beta}\right)\delta \quad (9) \end{aligned}$$

represent the switching points of the *optimal* bang-bang control. According to Eq. (5) the position $x_1(T^\star)$ is free, which yields the condition for the adjoint state variable

$$\lambda_1 = C_1 = 0. \quad (10)$$

Consequently, the first switching point ($\sigma(t_1) = 0$) calculates to

$$t_1 = -\sqrt{\frac{\alpha}{\beta}}\arctan\left(\frac{C_3}{C_2}\right), \quad (11)$$

which means that at $t = 0$ the input is set to $u = 1$ and oil flows through the valve until the switching point t_1, where the valve is shut. Substituting the initial condition $\mathbf{x}_0$ and Eq. (11) into the analytical solution Eq. (6) results in the initial condition $\mathbf{x}(t_1)$ for the second switching interval $t_1 < t < t_1 + t_2$.

Considering the control input $u \in [-\gamma, 0, 1]$ with $\gamma \geq 0$ yields the next switching interval

$$t_2 = T^\star - t_1 = -\sqrt{\frac{\alpha}{\beta}}\vartheta \text{ with} \quad (12)$$

$$\vartheta = \arctan\left(\frac{C_3}{C_2\left(\gamma\sqrt{\frac{C_3^2+C_2^2}{C_2{}^2}} + \sqrt{\frac{C_3^2+C_2^2}{C_2{}^2}} - 1\right)}\right)$$

Substituting Eq. (12) into the velocity equation from (6) and, furthermore, using the end condition $x_2(T^\star) = \frac{\delta}{\beta}$, then the relation for C_3 follows to

$$C_3 = -C_2\sqrt{4\gamma^2 + 8\gamma + 3}. \tag{13}$$

Substituting now Eq. (13) into Eq. (11) and Eq. (12) yields

$$t_1 = \sqrt{\frac{\alpha}{\beta}}\arctan\left(\sqrt{4\gamma^2+8\gamma+3}\right) \tag{14}$$

$$t_2 = \sqrt{\frac{\alpha}{\beta}}\arctan\left(\frac{\sqrt{4\gamma^2+8\gamma+3}}{2\gamma^2+4\gamma+1}\right), \tag{15}$$

which means that the drive is accelerated to maximum speed with two switching incidents. Thus, the resulting control reads

$$u = \begin{cases} 1 & 0 < t \le t_1 \\ -\gamma & t_1 < t \le T^\star \\ 1 & t > T^\star. \end{cases} \tag{16}$$

As mentioned above, for a movement in the opposite direction the control (16) can be inverted easily to $u^- = -u$.

2.2.1 Push Strategy

In this case the input flow rate is restricted to the interval $u \in [0, 1]$, which means that no second (tank sided) valve is used ($\gamma = 0$) for an extending movement. Thus, the switching points according to Eqs. (14) and (15) simplify to

$$t_1 = t_2 = \frac{\pi}{3}\sqrt{\frac{\alpha}{\beta}} \tag{17}$$

In the first switching interval the digital valve is opened for t_1 and in the second switching interval no further flow rate is supplied to the system, i.e. all valves are closed since $\gamma = 0$. At $T^\star = t_1 + t_2$ the maximum velocity of the drive is reached and from this time forward the digital “flow rate” is switched on again in order to maintain maximum steady state velocity of the drive. Since the conditions for optimality require $x_3(T^\star) = 0$, no pressure pulsations remain in the system. It is remarkable that in this case both switching times are identical and depend only on the natural frequency of the drive system. In contrast to that the velocity and, thus, the minimum position step are strongly related to the digital flow rate and, thus, to the valve size.

2.2.2 Push-Pull Strategy

Extending the input range to $u \in [-1, 0, 1]$, which accounts for a tank sided valve with the flow ratio $\gamma = 1$ with respect to the flow rate through the supply sided valve, yields the following switching points

$$t_1 = \sqrt{\frac{\alpha}{\beta}}\arctan\left(\sqrt{15}\right) \text{ and} \tag{18}$$

$$t_2 = \sqrt{\frac{\alpha}{\beta}}\arctan\left(\frac{\sqrt{15}}{7}\right). \tag{19}$$

Also in this case the points of switching only depend on the eigenvalues of the drive system. Compared to the push strategy the push-pull switching marginally lowers the response time $T^\star$ of the drive.

3 Simulations

The HDDC according to Eq. (16) was tested by numerical simulations in *Matlab/Simulink*. The simulation parameters of the configuration with regard to Fig. 1 are related to a common hydraulic cylinder drive and listed in Tab. 1. The input flow rate Q_V is related to a valve with $5\,\ell/\text{min}$ nominal flow rate at a pressure drop of 5 bar. The cross-section ratio of the cylinder areas is approximately one half, thus, the mean load pressure is half the supply pressure. In this context the input flow rate from Tab. 1 is justified for both digital valves.

In a first step the basic effect of the derived digital switching control is investigated by simulations employing the linearized model, which was used for the development of the HDDC. Later in another section advanced simulation experiments show the performance of the HDDC under more realistic conditions with regard to switching time of the valves, pipe line dynamics and friction.

3.1 Basic Simulation Experiments

In this section simulation results with the linearized model according to Eq. (2) are presented in order to demonstrate the basic performance of the HDDC derived above. For comparison reasons no friction is considered in the following simulations, which is in fact not realistic, but the effectiveness can be demonstrated more clearly.

Parameter	Value
cross section area of piston	$A_1 = \frac{53^2\pi}{4}\,\mathrm{mm}^2$
annulus cross section area	$A_2 = \frac{(53^2-36^2)\pi}{4}\,\mathrm{mm}^2$
cylinder length	$l_C = 0.5\,\mathrm{m}$
dead mass	$m = 500\,\mathrm{kg}$
initial piston position	$x_0 = 0.25\,\mathrm{m}$
piston sided dead volume	$V_{0A} = \left(0.1e^{-3} + A_1 x_0\right)\,\mathrm{m}^3$
annulus sided dead volume	$V_{0B} = \left(0.1e^{-3} + A_2\left(l_C - x_0\right)\right)\,\mathrm{m}^3$
bulk modulus of the fluid	$E = 1.2e^9\,\frac{\mathrm{N}}{\mathrm{m}^2}$
supply pressure	$p_S = 200\,\mathrm{bar}$
input flow rate	$Q_V = 5\sqrt{\frac{100}{5}}\,\frac{\ell}{\mathrm{min}}$

Tab. 1: System parameters

3.1.1 Push Strategy

In Fig. 2 the simulation results of the HDDC according to Eq. (17) and a single pulse control are compared. In Fig. 2a an exemplary ramp movement is depicted, where after acceleration the drive moves at steady state velocity for a certain distance and then decelerates with the inverted switching pattern.

In Fig. 2b the minimum step is illustrated, where the acceleration pattern is directly followed by the deceleration pattern. In both cases the input signals, of the HDDC and of the single pulse control, correspond to the same displacement volume of the drive. It can be seen that with the single pulse control large resonances are excited because no drive dynamics and are considered.

With the HDDC a certain minimum step size can be performed. Smaller steps can be realized with the double pulse strategy as presented, for instance, in [15]. In Fig. 3 the minimum HDDC step is opposed with a smaller step according to the double pulse concept. Combining both concepts, the HDDC and the double pulse strategy, result in arbitrary step sizes. Valve dynamics do not limit the minimum step size, since a double pulse movement can be also realized properly in a ballistic valve operation.

3.1.2 Push-Pull Strategy

In Fig. 4 the *push* and the *push-pull* strategy are opposed. The push-pull strategy achieves a slightly lower minimum step size due to the larger range of the control input. However, the difference is only marginal, since the response depends strongly on the dynamics of the drive.

3.1.3 Pulse Frequency Modulation

Basically, the HDDC is designed to accelerate the drive to maximum velocity and vice versa. If the acceleration pattern is immediately followed by the corresponding pattern for braking, then the minimum step size is achieved. In order to control a stepwise movement with a quasi mean velocity a certain sequence of individual velocity pulses must be generated. Here, only the push strategy is presented. In Fig. 5a simulation results of a frequency modulated velocity (FM) is depicted, where a sequence of several minimum position steps are commanded at different frequencies, which result in different mean velocities $\overline{v}$. The maximum quasi mean velocity, respectively, the maximum frequency is limited to $f_{max}^{FM} = \frac{1}{2T^\star}$. At higher pulse frequencies the control signals of the individual pulses would overlap, which is not intended here. Higher quasi mean velocities than with pure FM can be achieved by an additional variation of the pulse width, like depicted in Fig. 5b, which results in a Pulse-Frequency-Modulation (PFM). The maximum velocity is represented by $u = 1 = \mathrm{const}$, which is limited by the valve size and the operating pressure.

3.2 Advanced Simulations

In this section the influence of certain non-ideal effects on the system behavior are considered in

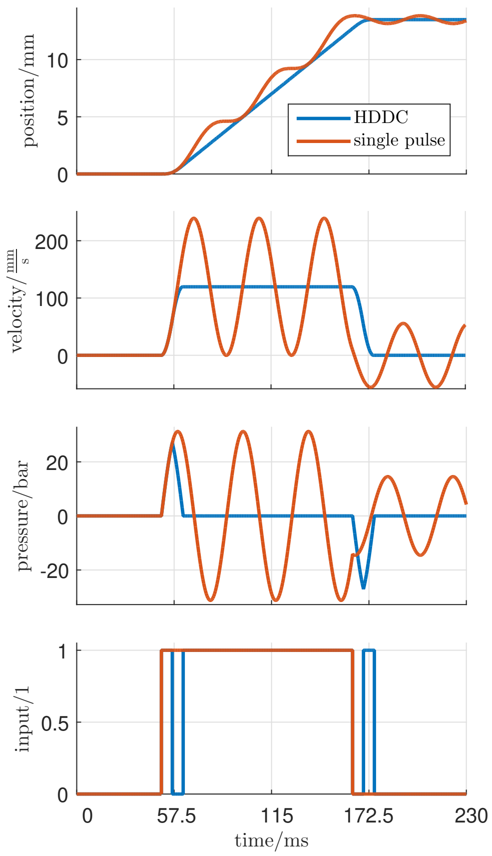

(a) Ramp movement

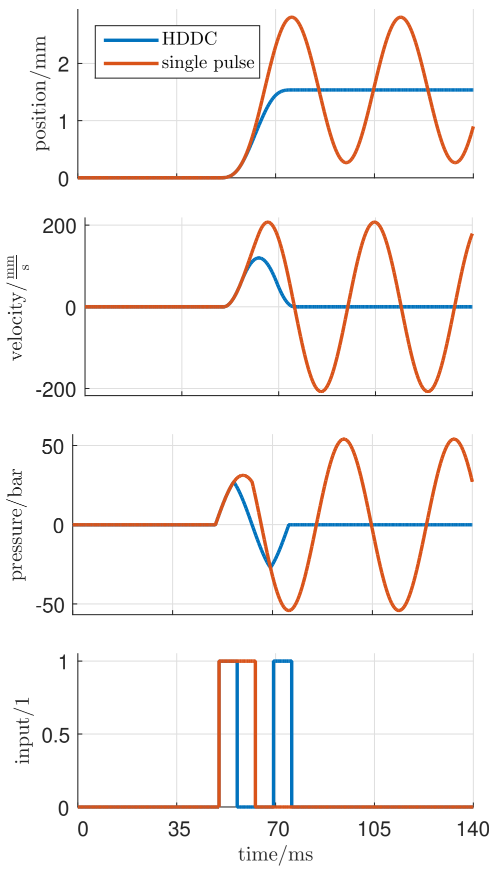

(b) Position step

Fig. 2: HDDC vs. single pulse

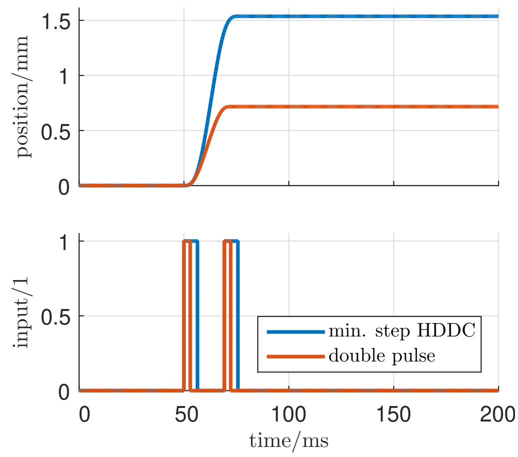

Fig. 3: Minimum step of the HDDC and smaller step with double pulse strategy

the simulations. With regard to a stepwise increase of complexity the simulations of the first non-ideal effect, the switching dynamics of real valves, are still carried out with the simple linearized model. Later on, the dynamics of a single pipe line are considered, additionally. The pipe model is based on a linear method of characteristics incorporating linear wave propagation effects in the transmission line according to [21, 22]. In a last step, simulations with the nonlinear model according to Eq. (1) incorporating a pipe line, switching dynamics and square root characteristics of the valves and friction are presented.

3.2.1 Influence of the Switching Time of the Valve

Real digital hydraulic valves do not switch instantaneously due to electronic delay, solenoid current build up and the inertia of the spool or poppet, thus, valves have a certain switching characteristics. Since the HDDC is an open loop concept a certain delay characteristics can be anticipated by the control algorithm. In this contribution the switching dynamics of the digital valves is modeled by a limited slope of the valve opening. In Fig. 6a the influence of two different valve switching times t_r on the drive response is shown. If the switching time of the valve is lower than the necessary pulse width required by the HDDC (in this case $t_r = 5\,\mathrm{ms} < t_1 = 6.4\,\mathrm{ms}$), then the control seems to work properly, since no significant pulsations occur in the response. At larger switching times (in this example $t_r = 10\,\mathrm{ms} > t_1 = 6.4\,\mathrm{ms}$)

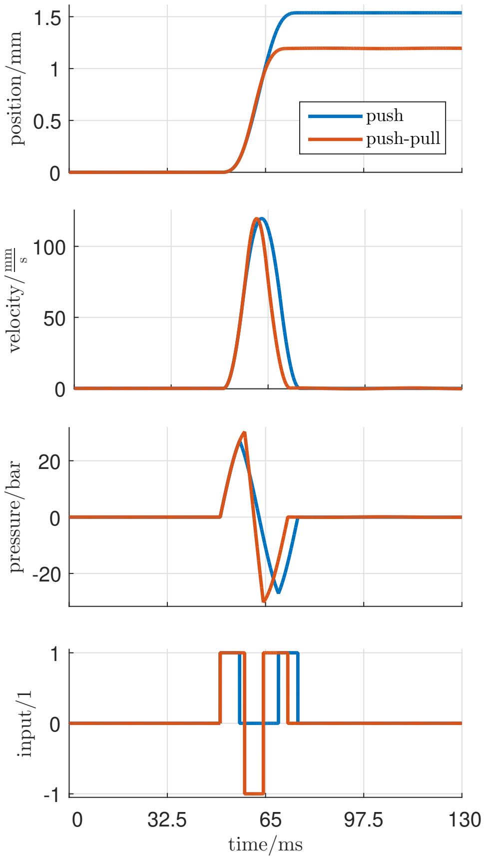

(a) Minimum step

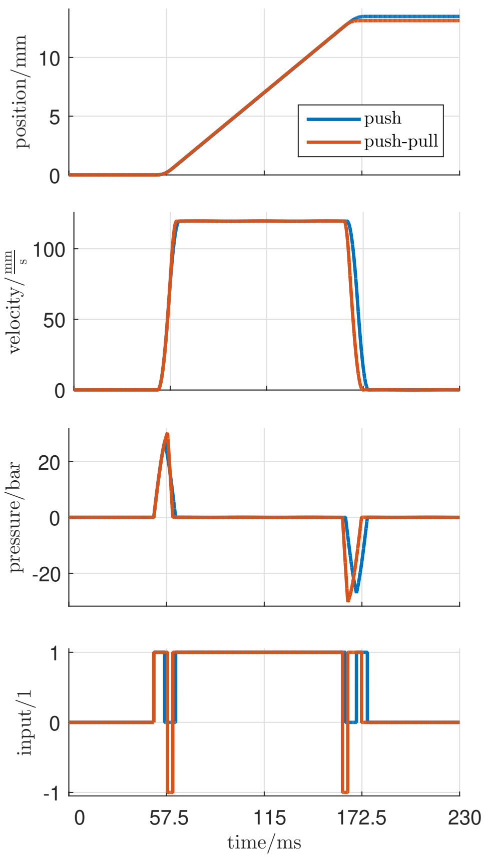

(b) Ramp movement

Fig. 4: Comparison of push and push-pull strategy

the HDDC is not able to completely compensate the drive dynamics anymore. The reason for this behavior is not investigated in detail in this contribution, however, this effect may be caused by an unsymmetrical partitioning of the energy for acceleration and freewheeling. In this specific case a correction of the switching times according to

$$\tilde{t}_1 = \frac{1}{2}\left(\frac{1}{2}T^\star + t_r\right) \tag{20}$$

$$\tilde{t}_2 = \frac{1}{2}T^\star \tag{21}$$

with the valve switching time t_r leads to a significant improvement of the system performance in case of large switching times, as shown in Fig. 6b. In this study symmetric switching characteristics are considered, which means that rise time and fall time are identical. But this cannot be expected in general. Therefore, in real applications the switching times $\tilde{t}_1$ and $\tilde{t}_2$ must be identified. Furthermore, due to wear of components over their life span an ongoing optimization of the switching times $\tilde{t}_1$ and $\tilde{t}_2$ must be expected.

3.2.2 Pipe Line Dynamics

In most linear drive applications the switching valves are not directly situated at the actuator, rather they are connected via pipes, like depicted in Fig. 7. According to expected wave propagation effects in the fluid due to the switching process the dynamics of transmission lines are additionally considered in the design of the HDDC. The model

$$\begin{bmatrix} p_j \\ q_j \end{bmatrix} = \begin{bmatrix} \cosh(\zeta l_P) & Z(s)\sinh(\zeta l_P) \\ -\frac{1}{Z(s)}\sinh(\zeta l_P) & \cosh(\zeta l_P) \end{bmatrix} \begin{bmatrix} p_i \\ q_i \end{bmatrix} \tag{22}$$

according to [23] with the pipe impedance $Z(s)$, the pipe length l_P and the frequency dependent wave coefficient ζ is often used for the consideration of linear wave propagation effects in transmission lines. With this model the pipe line dynamics can be efficiently calculated in frequency domain. After a suitable transformation of the model from Eq. (22) the pipe line dynamics can be easily considered in the state space representation of the

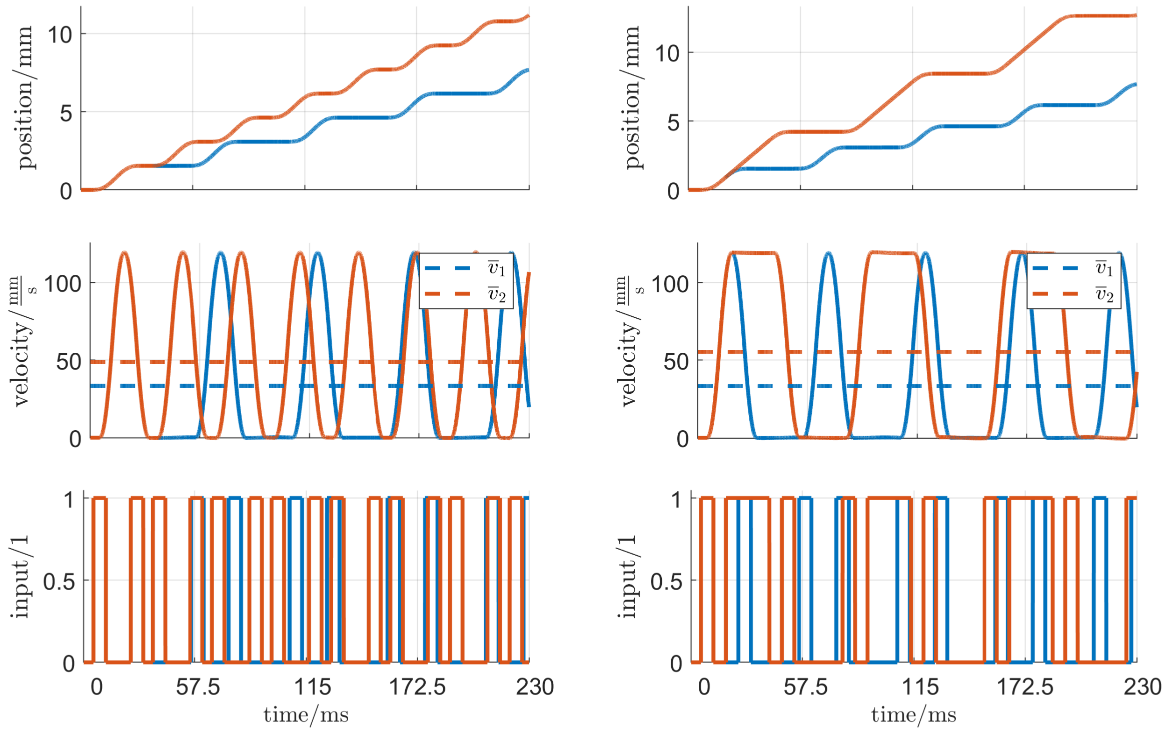

(a) Frequency-Modulation (b) Pulse-Frequency-Modulation

Fig. 5: Velocity control

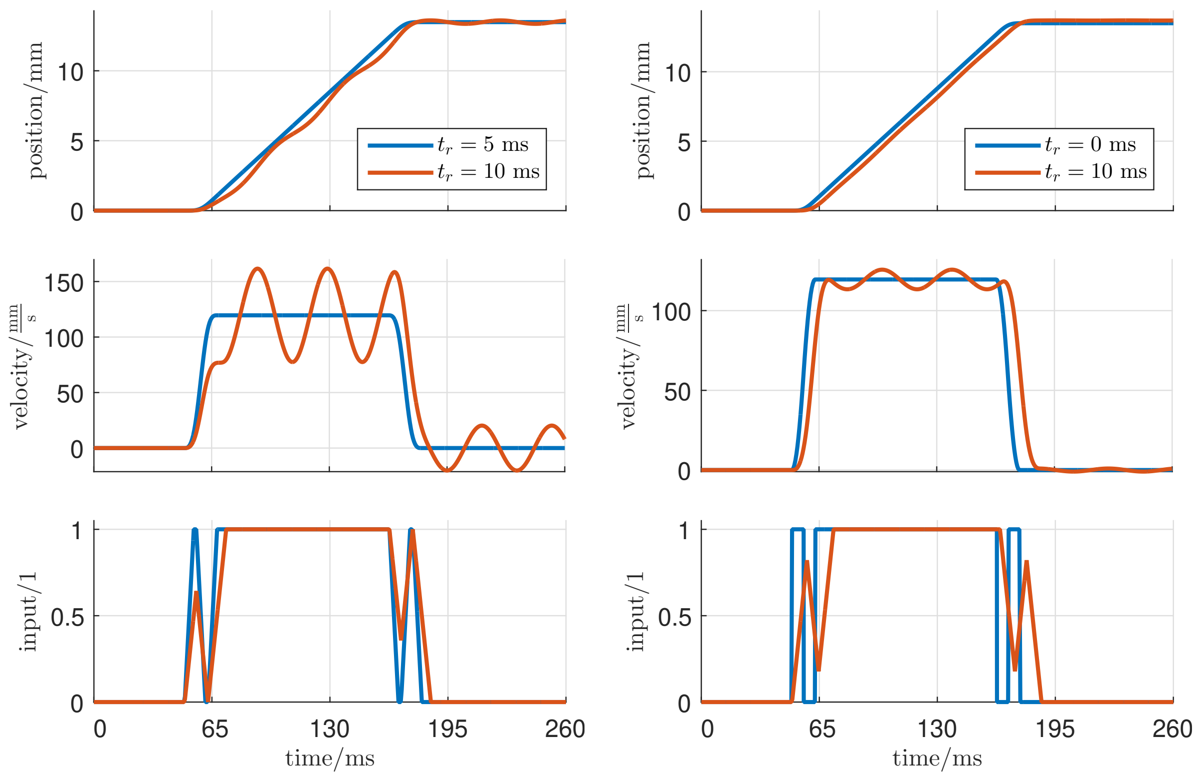

(a) Influence of valve dynamics (b) Compensation of valve dynamics

Fig. 6: Influence of the switching times of the valves

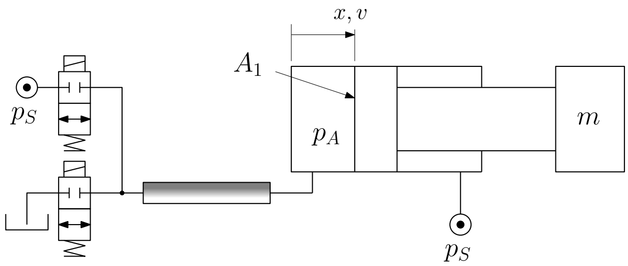

Fig. 7: HDDC considering pipe line dynamics

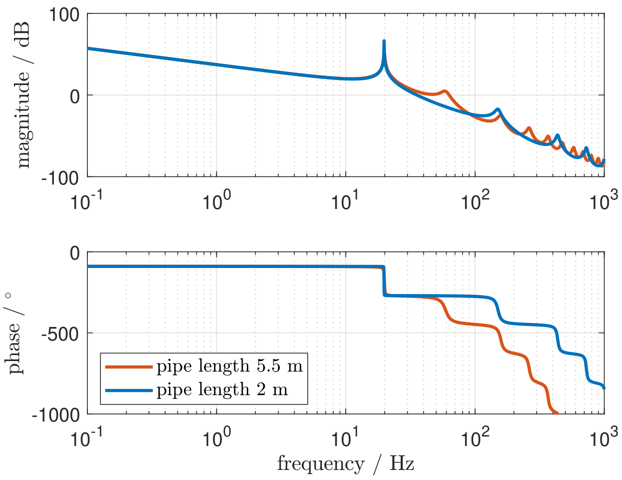

Fig. 8: Transfer function according to Eq. (24) for 2 different pipe lengths

linearized cylinder model of Eq. (2) in frequency domain, which results in

$$s\begin{bmatrix}\widehat{x}\\ \widehat{v}\\ \widehat{p_A}\end{bmatrix}=\begin{bmatrix}0 & 1 & 0\\ 0 & 0 & \frac{A_1}{m}\\ 0 & -\frac{EA_1}{V_C} & -\frac{E\sinh(\zeta l_P)}{V_C Z\cosh(\zeta l_P)}\end{bmatrix}\begin{bmatrix}\widehat{x}\\ \widehat{v}\\ \widehat{p_A}\end{bmatrix} + \begin{bmatrix}0\\ 0\\ \frac{E}{V_C\cosh(\zeta l_P)}\end{bmatrix}\widehat{q}\,(s)\,. \tag{23}$$

Thus, the transfer function of the position of the dead load according to the input flow rate reads

$$G\,(s)=\frac{\widehat{x}\,(s)}{\widehat{q}\,(s)}= \frac{EA_1}{s\left(\left(s^2 V_C m + EA_1^2\right)\cosh\left(\zeta l_P\right)+s\frac{Em}{Z}\sinh\left(\zeta l_P\right)\right)} \tag{24}$$

which is depicted in Fig. 8. The system parameters are the same as before according to Tab. 1. Furthermore, a pipe with 2 m in length and an inner diameter of $d_p = 20\,\mathrm{mm}$ is considered. Due to the pipe dynamics the transfer function has several natural frequencies. The first resonance at approximately 20 Hz represents the dynamics of the hydro-mechanic spring mass oscillator incorporating the dead mass and the oil stiffness in the piston sided cylinder chamber. The higher resonances are caused by the pipe line. The HDDC is designed to the first natural frequency of the transfer function from Fig. 8, because it is the dominant resonance peak ($> 0\,\mathrm{dB}$), which is intended to be compensated. All other eigenvalues are not considered in the design of the HDDC. However, it is not sufficient to completely neglect the pipe line in the transfer function, because also the dominant natural frequency of the spring mass oscillator is somewhat influenced by the pipe line dynamics.

In Fig. 9 simulation results of the drive responses for different movements are depicted. In this case the nonlinear cylinder dynamics according to Eq. (1) incorporating the mentioned pipe line were simulated. Furthermore, a valve switching time of $t_r = 5\,\mathrm{ms}$ was considered. The simulation results show that the digital valve control designed to the relevant natural frequency lead to a satisfying performance. Resonances of higher order do not play a significant role, at least in this case. On the one hand, this kind of robustness can be explained by the fact that all higher resonances show a significant lower peak than the design frequency. On the other hand, the limited switching dynamics of the digital valve even impedes a noticeable excitation of the higher resonances of the pipe line. The influence of the pipe line dynamics can be observed at the pressure signals. In the next to the lowest diagrams of Fig. 9 the two pressure signals indicate the pressure in the cylinder and at the valve. The end of the pipe, which is connected to the cylinder, has a pressure boundary with respect to the cylinder pressure. The other end of the pipe is connected to the valve, where the pressure shows fluctuations with a higher frequency, which were excited by the switching process. The observed frequency of approximately 150 Hz can be found as the second resonance peak of the system with the 2 meters pipe in the frequency plot of Fig. 8. Due to the mode shape of this resonance the pressure fluctuations have their maximum at the valve and their minimum in the cylinder. Thus, they do not influence the velocity response, significantly.

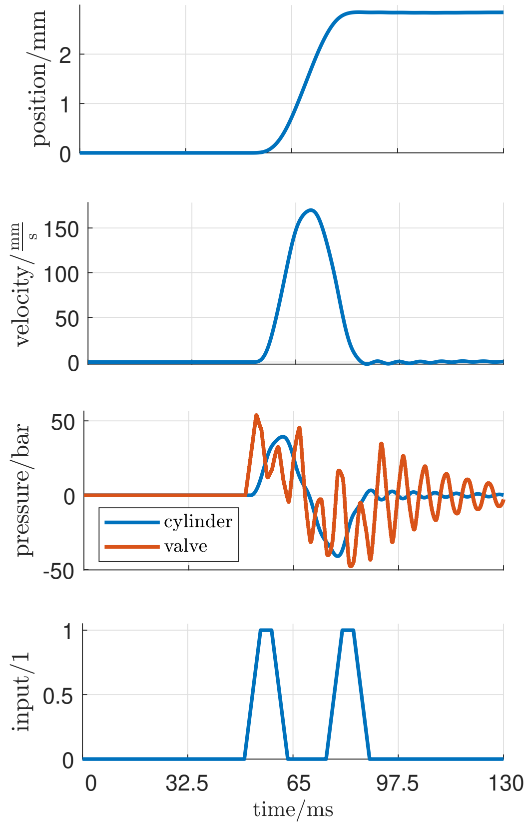

(a) Position step

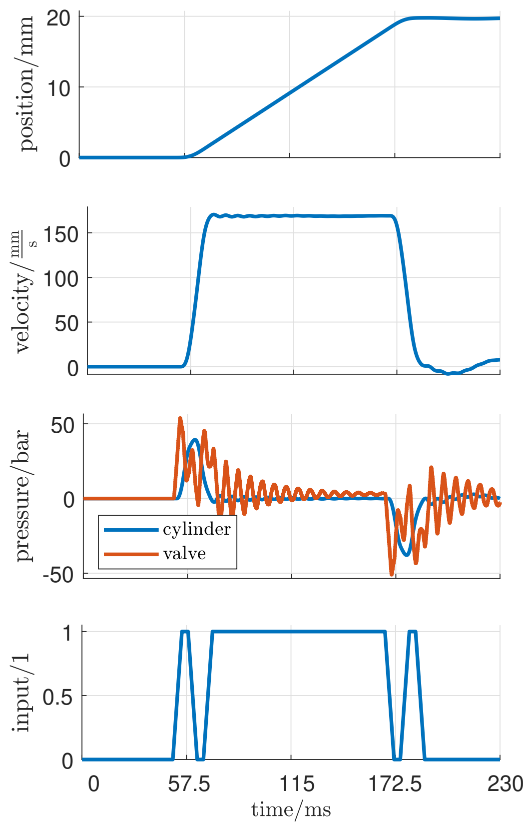

(b) Ramp movement

Fig. 9: System responses considering a pipe line of 2 meters in length

All higher resonances do not show up in the results of Fig. 9 due to the limited excitation band width.

The design of the HDDC is related to the first natural frequency of the system, which is sufficient for many hydraulic drive applications, since the switching dynamics of the digital valves represent a reduced excitation of higher resonances. In the presented case of the push strategy, the ON and OFF switching times of the HDDC are identical, as shown in Eq. (17). Thus, the desired time domain input (flow rate) signal has a high spectral content at the frequency $\widetilde{\omega} = 3\sqrt{\frac{\beta}{\alpha}}$. Thus, the second natural frequency of the system must have a significant distance to $\widetilde{\omega}$ in order to avoid unwanted vibrations. In the particular case the pipe line between the valve and the cylinder must not have its first resonance peak in the range of the triple design frequency, which is a restriction for the dimension of the used transmission line. In order to demonstrate this effect, simulation results of a system with an uncritical and, respectively, with a critical pipe length are opposed in Fig. 10. The simulation results show large fluctuations in pressure and velocity due to the resonance peak of the longer pipe (5.5 m) at the critical frequency $\widetilde{\omega} = 3\sqrt{\frac{\beta}{\alpha}}$ according to the frequency plot from Fig. 8.

3.2.3 Friction

The digital valve control according to Eq. (16) is developed completely without damping, which made the derivation much more easier. However, in reality considerable friction must be expected. For the simulation experiments presented in the following a static friction model according to Fig. 11a was used, including a stick-slip effect. The parameters of the friction model were approximated in accordance with a real test bench of an identical dimension. Furthermore, in the simulations the square root characteristics of the switching valves with a nominal size of $Q_N \approx 5\,\frac{\ell}{\text{min}}$@5bar were considered. The results are depicted in Fig. 11b, where the red curve shows the response due to a single pulse actuation and the blue curve the performance with regard to the derived digital valve control according to Eq. (17). It can be seen that with the presented digital valve actuation a significant reduction of the resonances

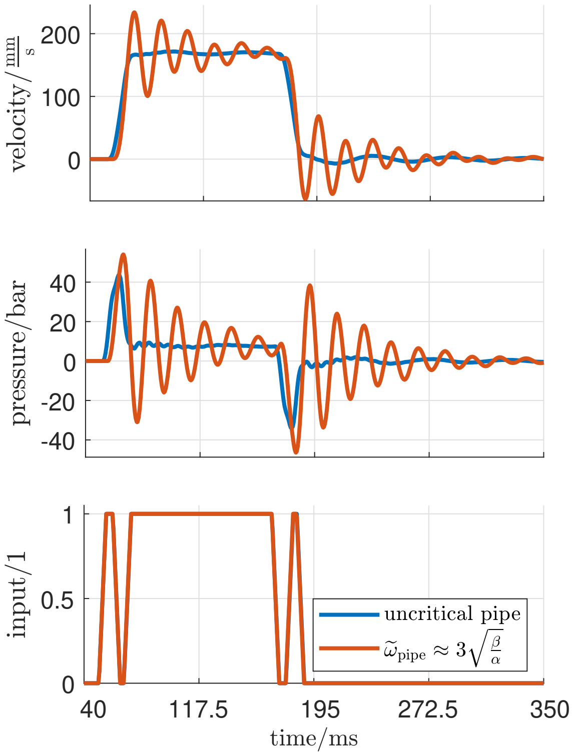

Fig. 10: Influence of pipe dynamics

can be achieved. The performance can be even improved if the switching events t_1 and t_2 are corrected within a few tenths of a millisecond by optimization. Such a result is shown by the yellow curve, however, the optimizing process is out of the scope of this article. Depending on the desired accuracy, nonlinear friction effects like stick-slip, dry friction and the Stribeck effect seem to play an inferior role in such a weakly damped hydraulic drive system, since an adaption of the switching times in the range of a few milliseconds is sufficient to compensate the deviation resulting from friction. In this case the resulting acceleration due to the rapid valve switching overrides the stick-slip effect and, furthermore, the occurrent friction does not significantly influence the resonance effect at the dominating natural frequency of the drive system. However, since only one specific drive configuration was investigated by simulation, further work must be devoted to this issue.

4 Discussion

The HDDC represents certain switching patterns in order to accelerate and decelerate the drive system. If the ON-pattern is directly followed by the OFF-pattern the minimum position step is performed. For smaller steps the method coincides with the double pulse strategy according to literature, as for instance in [15]. The minimum steps can be realized arbitrary consecutively, which represents a sort of stepper drive. The step size depends on the size of the switching valve and on the load pressure. Furthermore, if the OFF-pattern is delayed for a certain time arbitrary large steps at maximum velocity can be achieved. Thus, the steps size and the step frequency can be controlled, which results in a Pulse-Frequency-Modulation (PFM) for digital hydraulic drives.

Actually, the HDDC is an open loop concept, however, it is simple to realize a closed loop three-level controller for the piston position. Furthermore, if the necessary distance for deceleration is anticipated, then a remarkable accuracy can be achieved. In such a case the natural frequency must be known in every desired target position, since the dynamics of the drive depends on the position of the piston.

For a proper operation of the HDDC the used digital valves have to meet certain requirements on their minimum switching time. In case of slower valves a correction of the switching patterns can be done in order to achieve the most intended effect on the drive's response. It must be expected that due to wear effects on real applications the switching pattern must be corrected also during operation in order to achieve the desired behavior over the life span of the drive system.

In fact, the achievable accuracy strongly depends on the dynamics of the switching valves, but also on the sampling rate of the signal processing unit, where the controller is implemented. Since the first natural frequency of some realistic hydraulic drive systems can go up to the order of 100 Hz, the characteristic switching signals must be performed in the range of a few milliseconds. Thus, for an optimal drive performance the switching events must be timed within some tenths of a millisecond, which only can be achieved with a signal processing unit running on a sufficiently small sample time.

So far, no variations of the dead mass and the load force were considered in the investigations. On the one hand it is clear that the dead mass m has significant influence on the drive's natural frequency $\omega = \sqrt{\frac{\beta}{\alpha}} = \sqrt{\frac{EA_1}{mx}}$. Thus, in case of different dead

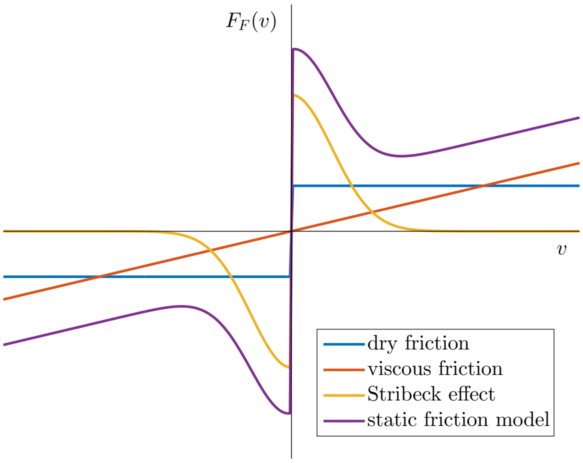

(a) Static friction model

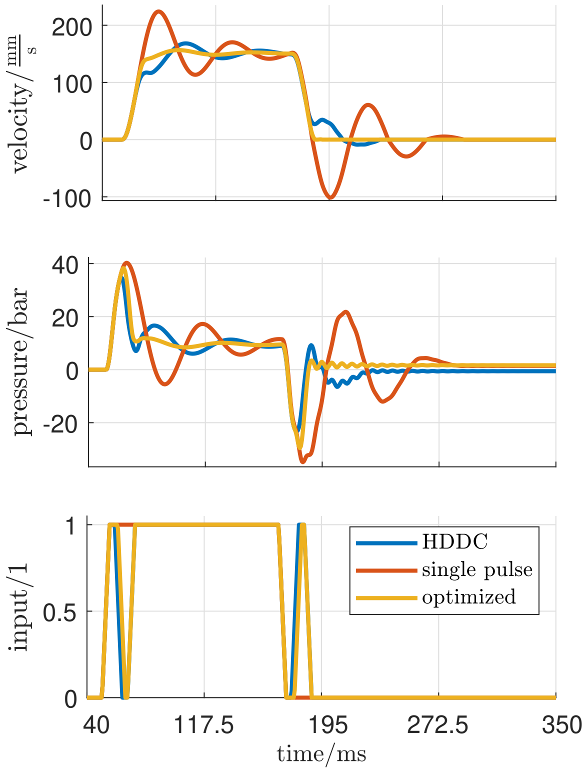

(b) Influence of static friction

Fig. 11: Simulations considering valve characteristics, pipe line dynamics and friction

loads the mass must be either known or somehow identified. On the other hand unknown *constant* load forces are expected to have no significant influence on the desired response, since they only result in a different mean pressure in the chamber of a single actuated cylinder. However, variations of the load force seem to be critical during the acceleration and deceleration phase. Since the load force is often a result from the interaction with a dynamic load system, a constant load force cannot be assumed a priori. Thus, variations of the load will represent a major topic in further investigations.

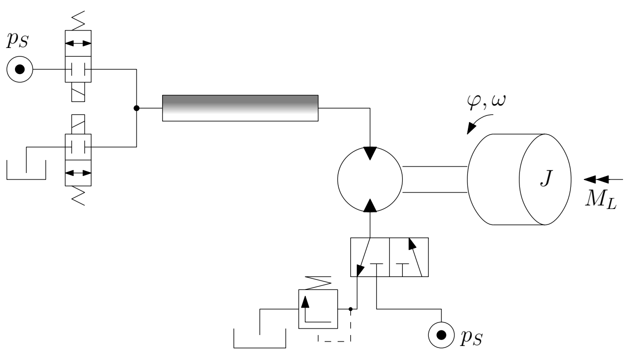

Fig. 12: Rotary hydraulic drive qualified for an HDDC in both moving directions

The HDDC represents a bang-bang control for a class of digital hydraulic systems, in particular, single chamber actuated drives. Since the control is designed to the transfer function of the complete system comprising the inertia of the dead load, the compressibility of the fluid in the cylinder chambers and the pipe line dynamics. In real applications the necessary transfer function must be identified by simple measurements or may be approximated already in the design process. Basically, the application of the HDDC is not restricted to cylinder drives and, thus, can be also employed for rotary drives like, for instance, depicted in Fig. 12.

5 Conclusion and Outlook

The presented HDDC is an open loop concept, which is designed to the dynamics of the drive system. With the HDDC the maximum physical dynamic response of the hydraulic drive can be achieved and unwanted resonances can be reduced to a minimum. If the digital hydraulic drive system has only one eigenfrequency no oscillations remain after the intended movement. Furthermore, with the HDDC a sort of step control can be realized, which may be qualified for a position control without any position sensor for certain applications. The step size depends on the size of the used digital valves and, furthermore, on the load pressure. However, an operation without any position sensor requires at least knowledge of the load conditions. It must be expected that an ideal switching cannot be realized in real applications. Therefore, the switching pattern must be optimized during operation in order to achieve the desired performance. Future work will focus on testing the presented HDDC on a real drive system, where also the robustness with regard to different load conditions will be investigated.

Acknowledgment

This work has been supported by the Austrian COMET-K2 programme of the Linz Center of Mechatronics (LCM), and was funded by the Austrian federal government and the federal state of Upper Austria.

References

[1] M. Linjama, M. Vilenius, Digital Hydraulics - Towards Perfect Valve Technology, in: J. Vilenius, K. T. Koskinen (Eds.), Proceedings of The 10^{th} Scandinavian Interational Conference on Fluid Power, SICFP'07, May 21-23, Tampere, Finland, Vol. 1(3), Tampere University of Technology, 2007, pp. 181–196.

[2] M. Linjama, Digital Hydraulics Research at IHA, in: Proceedings of The 1^{st} Workshop on Digital Fluid Power, 3^{rd} October, Tampere, Finland, 2008.

[3] M. Linjama, Digital Fluid Power - State of the Art, in: 12^{th} Scandinavian Interational Conference on Fluid Power, SICFP'11, May 18-20, Tampere, Finland, Vol. 3(4), 2011, pp. 331–353.

[4] L. Hanxiu, Y. Yuqing, Xuli, The PWM Electrohydraulic Control System Using A Computer, Tech. rep., Zhejiang University (1987).

[5] R. Scheidl, D. Schindler, G. Riha, W. Leitner, Basics for the Energy-Efficient Control of Hydraulic Drives by Switching Techniques, in: J. Lückel (Ed.), Proceedings of the Third Conference on Mechatronics and Robotics, Vieweg+Teubner Verlag, 1995, pp. 118–131. doi:10.1007/978-3-322-91170-4_9.

[6] B. Winkler, K. Ladner, H. Kogler, R. Scheidl, Switching Control of a Linear Hydraulic Drive - Experimental analysis, in: Proceedings of the 9^{th} Scandinavian International Conference on Fluid Power, Linköping, Sweden, 2005.

[7] R. Scheidl, B. Manhartsgruber, State of the Art in Hydraulic Switching Control - Components, Systems, Applications, in: Proceedings of the 9^{th} Scandinavian International Conference on Fluid Power, SICFP '05, Linköping, Sweden, June 1-3, 2005, ext. abstracts vol.1, p.46.

[8] A. Hießl, A. Plöckinger, B. Winkler, R. Scheidl, Sliding Mode Control for Digital Hydraulic Applications, in: Proceedings of the 5^{th} Workshop on Digital Fluid Power, 2012.

[9] H. Kogler, R. Scheidl, Two Basic Concepts of Hydraulic Switching Converters, in: Proceedings of the First Workshop on Digital Fluid Power, DFP08, Tampere, Finland, 2008.

[10] N. D. Johnston, A Switched Inertance Device for Efficient Control of Pressure and Flow, in: ASME 2009 Dynamic Systems and Control Conference, Volume 1, ASME, 2009, pp. 589–596, doi:10.1115/DSCC2009-2535. doi:10.1115/dscc2009-2535.

[11] H. Kogler, R. Scheidl, The Hydraulic Buck Converter exploiting the Load Capacitance, in: 8^{th} IFK - "Fluid Power Drives", $26^{th}-28^{th}$ March, Dresden, Germany, Vol. 2(3), 2012, pp. 297–309.

[12] M. Pan, N. Johnston, A. Plummer, S. Kudzma, A. Hillis, Theoretical and Experimental Studies of a Switched Inertance Hydraulic System, Proceedings

of the Institution of Mechanical Engineers, Part I: Journal of Systems and Control Engineering 228 (1) (2013) 12–25. doi:10.1177/0959651813500952.

[13] V. J. D. Negri, P. Wang, A. Plummer, N. D. Johnston, Behavioural Prediction of Hydraulic Step-Up Switching Converters, International Journal of Fluid Power 15 (1) (2014) 1–9. doi:10.1080/14399776.2014.882057.

[14] R. Scheidl, B. Steiner, B. Winkler, G. Mikota, Basic Problems in Fast Hydraulic Switching Valve Technology, in: Proceedings of the 6^{th} International Conference on Fluid Power Transmission and Control (ICFP05), Hangzhou, China, 2005.

[15] C. Gradl, R. Scheidl, A Basic Study on the Response Dynamics of Pulse-Frequency Controlled Digital Hydraulic Drives, in: ASME/BATH 2013 Symposium on Fluid Power and Motion Control, ASME, 2013. doi:10.1115/fpmc2013-4438.

[16] R. Haas, E. Lukachev, Optimal Feedforward Control of a Digital Hydraulic Drive, in: Proceedings of the 7^{th} Workshop on Digital Fluid Power, DFP15.

[17] R. Haas, C. Hinterbichler, E. Lukachev, M. Schöberl, Optimal Digital Hydraulic Feed-Forward Control applied to Simple Cylinder Drives, in: Proceedings of the 8^{th} Workshop on Digital Fluid Power, May 24-25, Tampere, Finland, 2016.

[18] J. Macki, A. Strauss, Introduction to Optimal Control Theory, Springer, 1982. doi:10.1007/978-1-4612-5671-7.

[19] W. E. Singhose, N. Singer, Design and Implementation of Time-Optimal Negative Input Shapers (1996).

[20] K. Sorensen, W. Singhose, S. Dickerson, A Controller Enabling Precise Positioning and Sway Reduction in Cranes with On-Off Actuation, in: Proceedings of the 16^{th} International Federation of Automatic Control World Congress, Prague, 2005. doi:10.3182/20050703-6-cz-1902.00497.

[21] W. Zielke, Frequency-dependent friction in transient pipes, ASME Journal of Basic Engineering 90(1) (1968) 109–115.

[22] K. Suzuki, T. Taketomi, S. Sato, Improving Zielke's method of simulating frequency-dependent friction in laminar liquid pipe flow, Journal of Fluids Engineering 113 (4) (1991) 569. doi:10.1115/1.2926516.

[23] A. F. D'Souza, R. Oldenburger, Dynamic response of fluid lines, Journal of Basic Engineering 86 (3) (1964) 589–598. doi:10.1115/1.3653180.

Nomenclature

A dynamic matrix

b input vector

C constant

$G(s)$ transfer function

H Hamiltonian

λ adjoint state variables

$\boldsymbol{\lambda}$ adjoint state vector

s laplace variable

σ switching function

u control input

x state vector

α auxiliary variable

β auxiliary variable

δ auxiliary variable

γ scaled valve size .... [1]

ω eigen values

Δp pressure drop .... $[Pa]$

ζ wave propagation coefficient .... $[1/m]$

A_1 cross-section area of piston .... $[m^2]$

A_2 annulus cross-section area .... $[m^2]$

d_v viscous friction .... $[Ns/m]$

E fluid compressibility .... $[Pa]$

f frequency .... $[1/s]$

l_C cylinder length .... $[m]$

m dead mass .... $[kg]$

p pressure .... $[Pa]$

p_A load pressure .... $[Pa]$

p_N nominal pressure drop .... $[Pa]$

p_S supply pressure .... $[Pa]$

q flow rate .... $[m^3/s]$

Q_N nominal flow rate .... $[m^3/s]$

Q_V flow rate through valve .... $[m^3/s]$

t time .... $[s]$

t_r valve switching time .... $[s]$

$T^\star$ optimal time .... $[s]$

v velocity .... $[m/s]$

V_0 dead volume .... $[m^3]$

x position .... $[m]$

Z pipe impedance .... $[\frac{kg}{m^4 s}]$

List of Figures

List of Tables